Dynamic Observation for Reaction Propagation in Lithium-Ion Battery Cathode by Means of VDXAFS Technique

Hirona Yamagishi, Ryota Miyahara, Misaki Katayama, and Yasuhiro Inada

Department of Applied Chemistry, Graduate School of Life Sciences, Ritsumeikan University, 1-1-1 Noji-Higashi, Kusatsu, Shiga 525-8577, Japan

Abstract

The chemical state change in the lithium ion battery cathode has been analyzed by means of the VDXAFS technique for the $LiFePO_4$ or $LiMn_2O_4$ cathode. The VDXAFS measurement was carried out for the charging process after a rapid potential jump, and the space- and time-resolved XAFS data were collected simultaneously to observed the propagation of the electrode reaction. For both cases, the reaction channel where the electrode reaction preceded and the propagation of the electrode reaction from the reaction channel were directly observed for the operating battery. The propagation in the cathode sheet was modeled by an equation composed of a first-order rate equation to represent the electrochemical reaction at the reaction channel and an analogue of the solution of the diffusion equation to describe the propagation from the reaction channel. The observed data were reproduced by the model equation, and the electronic conductivity is then concluded to be an origin to generate the inhomogeneous progress of the electrode reaction.

1. Introduction

Lithium ion batteries (LIBs) are widely used as an energy storage device, and the development of the next-generation electrode material is continued to achieve the long life, the stable utilization, the high charge/discharge capacity, and the high-rate operation. The *in-situ* X-ray diffraction (XRD) [1] and *in-situ* X-ray absorption fine structure (XAFS) measurements [2] have demonstrated that the charge/discharge reaction for the $LiFePO_4$ cathode is a chemical conversion between the $LiFePO_4$ and $FePO_4$ phase. The domino-cascade model has been proposed to explain the lithiation and delithiation processes [3]. More recently, it has been reported the existence of an intermediate phase, Li_xFePO_4, during the high-rate charge/discharge processes by means of the time-resolved *in-situ* XRD technique [4]. In addition, the mismatch between the battery capacity and the chemical state of the Fe species estimated by the XRD and XAFS methods suggested the spatial inhomogeneity for the progress of the electrode reaction in the cathode plain [5]. Such the inhomogeneity means the existence of some reaction spots, at where the electrode reaction precedes, and the formation of the reaction spot involves an excess local current exceeding the operating average current. Such unfavorable excess current may cause some serious problems for the stable operation of the LIB, *e.g.*, the decomposition of the electrolyte solvent and the local temperature increase [6]. Because they might induce serious accidents like firing, it is necessary for the safe utilization of LIBs to understand the occurrence mechanism of the inhomogeneous reaction.

We have developed the methodology using XAFS to observe directly the inhomogeneous progress of the electrode reaction appeared in the cathode sheet of LIB. The XAFS method is powerful for observing the electrode reaction because it is sensitive to the chemical state of a target element and is able to apply nondestructively. By replacing the conventional detector to measure the transmission X-ray intensity with a two-dimensional (2D) detector, the space-resolved XAFS imaging technique has been established with the spatial resolution of the pixel size of the 2D detector [7]. We have directly demonstrated the inhomogeneous progress of the electrode reaction in the $LiFePO_4$ cathode sheet. Some positions, at where the electrode reaction precedes, named as “reaction channel”, have been clearly shown by the *in-situ* XAFS imaging measurements during the charging and discharging processes [8]. The result gave us an image of the electrode reaction as the propagation of the chemical state conversion from the reaction channel to the surrounding area. Furthermore, it is found that the addition of the amount of the conductive additive diminishes the inhomogeneous distribution at the same state of charge/discharge. It is thus concluded that the inhomogeneous progress due to the existence of the reaction channels is caused by the locally advanced electric conductively in the cathode sheet. On the contrary, the inhomogeneous progress is

not observed in the case of the $LiMn_2O_4$ cathode, and it is considered that the generated reaction channels may relax owing to the fast propagation to the surrounding area, leading to the average of the chemical state, during the single XAFS imaging measurement.

The inhomogeneous electrode reaction as observed for the $LiFePO_4$ cathode sheet using the XAFS imaging technique has been reported by the other methods, such as the X-ray fluorescence detection [9] and the Raman spectroscopy [10]. However, the fundamental essence to generate the inhomogeneous progress has not been clarified yet. In this study, we have applied the newly developed vertically dispersive XAFS (VDXAFS) technique [11] to observe dynamically the reaction progress in the cathode sheet during the charging and discharging processes under the operating conditions. Because the VDXAFS technique permits us to perform both the space- and time-resolved XAFS analysis, it is expected to analyze the propagation dynamics of the inhomogeneous electrode reaction appeared in the LIB cathode. The available aspects are useful to construct the stable LIB system without the local generation of excess current.

In this study, the chemical state change has been investigated using the VDXAFS technique for the $LiFePO_4$ and $LiMn_2O_4$ cathodes of LIB. The time-course change of the chemical state has been measured with the space and time resolution of 300 μm and 0.5 s, respectively, for the charging process after a jump of the cell voltage to a higher potential than that at which the oxidation of $LiFePO_4$ or $LiMn_2O_4$ takes place. The propagation processes of the electrode reaction for two active materials will be compared to understand the generation and relaxing mechanisms.

2. Experimental

The LIB cell for the VDXAFS measurement was assembled as the following procedures. The cathode slurry was prepared by mixing the cathode material, acetylene black as the conductive additive, and polyvinylidene difluoride as the binder material with the mass ratio of 14:3:3 and 15:3:2 for $LiMn_2O_4$ and $LiFePO_4$, respectively, and was applied onto an aluminum foil with the thickness of 100 μm. After pressing in air and drying in vacuum, the cathode sheet was cut to the size of 11 mm (horizontal) x 3 mm (vertical). The current collector tab was ultrasonically welded to the cathode sheet after a part of cathode material was removed. The LIB cell was composed of the cathode sheet, a Li foil anode, two polypropylene separators, and 1 mol dm^{-3} $LiPF_6$ solution dissolved in ethylene carbonate and ethyl methyl carbonate with the volume ratio of 3:7, and the all parts were enclosed in an envelope of aluminum laminated film.

The VDXAFS measurements at the Mn K edge for $LiMn_2O_4$ and the Fe K edge for

$LiFePO_4$ were conducted at BL-5 of SR center (Ritsumeikan University) and NW2A of PF-AR (KEK). The time-resolved measurement was triggered by a quick jump of the cell voltage to 4.5 V for $LiMn_2O_4$ and 4.2 V for $LiFePO_4$. The exposure time was 0.5 s to get one 2D image of the transmission intensity. The chemical state of the active material was determined using the X-ray energy at the white line peak for $LiMn_2O_4$ and at the absorption edge for $LiFePO_4$.

3. Results and Discussion

The time-course change of the chemical state at a measured line is shown in Fig. 1 and 2 for $LiFePO_4$ and $LiMn_2O_4$, respectively, during the charging process. The oxidized state of the active material with the higher valence state after the complete charge is denoted by the red pixel, while the reduced state before the charging process is shown by the blue pixel. For both cases, the Fe and Mn species had the lower valence state at the beginning of the measurement, and the whole area was converted to the higher valence state after the completion of the charging process at 2000 s. As observed by the 2D XAFS imaging measurement [8], the reaction spot where the charging reaction preceded was appeared at the position around 3 mm in the case of $LiFePO_4$ shown in Fig. 1. The similar phenomenon was observed in the case of $LiMn_2O_4$ (see Fig. 2) at the position around 4 mm. This is a first report to observe the inhomogeneous progress of the electrode reaction for $LiMn_2O_4$. It is thus implied that the VDXAFS technique is effective to detect dynamically the inhomogeneous distribution, which relaxes rapidly to be changed to the homogeneous state of charge. The present VDXAFS measurement clearly indicated the spatial propagation of the charging reaction from the reaction channel not only for $LiFePO_4$ but also for $LiMn_2O_4$.

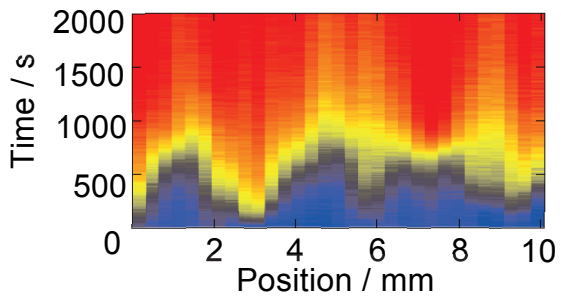

Fig. 1 The time-course change of the chemical state of Fe in $LiFePO_4$ cathode.

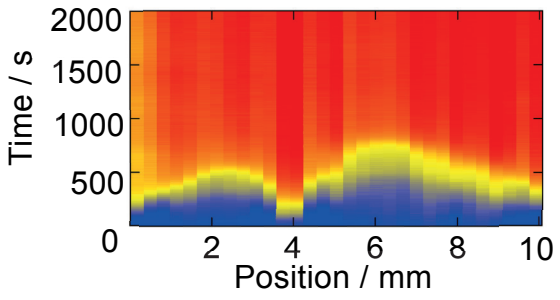

Fig. 2 The time-course change of the chemical state of Mn in $LiMn_2O_4$ cathode.

In order to model the spatial propagation to relax the inhomogeneous electrode reaction, a function composed of a first-order rate equation and an analogue of the solution of the diffusion equation was constructed as equation (1),

$$S(x,t) = \{1 - \exp(-kt)\} \times \{1 - \mathrm{erf}\left(\frac{x}{D't}\right)\} \qquad (1)$$

where S is the state of charge determined by the observed XAFS spectrum, x is the distance from the reaction channel, t is the time after the start of charge by a jump of the cell voltage, k is the first-order rate constant to represent the electrochemical reaction at the reaction channel, and D' is an analogue of the diffusion constant to explain the propagation of the electrode reaction from the reaction channel. The experimental result for $LiFePO_4$ shown in Fig. 1 was fitted using the equation (1), and the values of k and D' were determined to 2.0×10^{-3} s^{-1} and 3.9×10^{-2} mm s^{-1}, respectively. The experimental data and the calculated

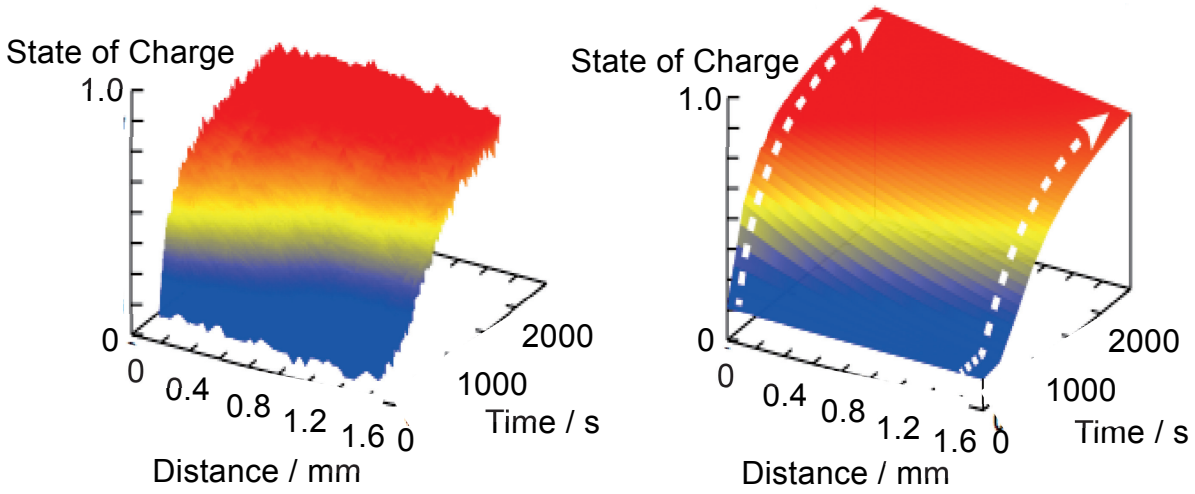

Fig. 3 The time-course change of the chemical state of Fe in $LiFePO_4$ at around the reaction channel (x = 0). The experimental data shown in the left figure is compared with the calculated result depicted using equation (1) shown in the right figure.

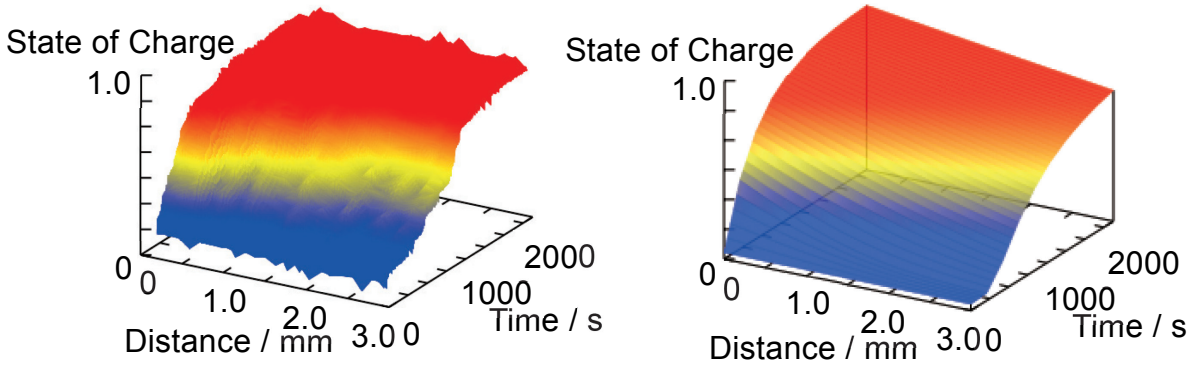

Fig. 4 The time-course change of the chemical state of Mn in $LiMn_2O_4$ at around the reaction channel (x = 0). The experimental data shown in the left figure is compared with the calculated result depicted using equation (1) shown in the right figure.

change of S using the optimized parameters are shown in Fig. 3 for the charging reaction of $LiFePO_4$. The origin of x (distance axis) in Fig. 3 corresponds to the reaction channel observed at the position around 3 mm in Fig. 1. The calculated data well reproduces the experimentally observed propagation of the electrode reaction. The same fitting procedure was conducted to the data of $LiMn_2O_4$, and the values of k and D' were successfully determined to 3.0×10^{-3} s^{-1} and 1.1×10^{-2} mm s^{-1}, respectively, as shown in Fig. 4, for which the origin of x (distance axis) corresponds to the reaction channel observed at the position around 4 mm in Fig. 2. The reaction propagation is properly reproduced by the model function of equation (2) also for the $LiMn_2O_4$ cathode. These facts clearly indicate that the electrode reaction in the cathode sheet is described using equation (2) in considering the electrochemical reaction at the reaction channel accompanied by the propagation along the spatial axis. It is then concluded that the inhomogeneous progress of the electrode reaction is caused by the same origin for both cases of the $LiFePO_4$ and $LiMn_2O_4$ cathode.

Figure 5 shows the schematic concept of the cross section of a cathode layer, which is composed of the conductive additive, *i.e.*, carbon particles denoted by black circles, which produces the conducting network for electrons, the void vacancy denoted by white circles, in which the electrolyte solution is filled and the Li ion is passed through, the particles of the active material, and the Al sheet as the current collector. This model assumes that the electronic conduction between the current collector and the cathode material is limited at the contact points between the carbon particle and the current collector, because the electric conductivity of the active material is significantly low in comparison to that of carbon. The electrically connected pathway can form by the carbon particles in the cathode layer, and the electrons transfer via the pathway during the charging and discharging processes. It is considered that some pathways pass through the cathode layer to reach to the interface with the electrolyte solution. Because the XAFS imaging and VDXAFS measurements are performed in the transmission mode, the chemical species in the X-ray light path are averaged and the positions at such electronic pathway becomes the reaction channel where the electrochemical reaction precedes. The electric resistance is thus considered to become larger when the position of an active material particle is distant from the reaction channel because of the degraded electronic conductivity. Such increased

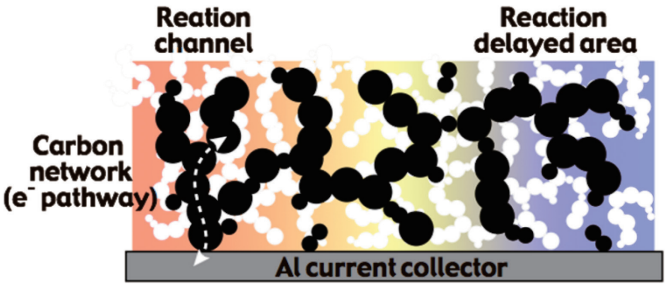

Fig. 5 The propagation model of the electrode reaction in the cathode sheet.

resistance causes the delay of the electrode reaction proportional to the distance from the reaction channel because of the drop of the effective potential. The present study has revealed that the electronic conductivity is an origin to generate the inhomogeneous progress of the electrode reaction in the cathode sheet of LIB.

4. Conclusions

The inhomogeneous progress of the electrode reaction has been investigated by the VDXAFS technique for the $LiFePO_4$ and $LiMn_2O_4$ cathode. The occurrence of the reaction channel where the electrochemical reaction preceded was observed during the constant voltage charging process for both cathode materials. The propagation of the electrode reaction from the reaction channel to the surrounding area was analyzed using the model function composed of a first-order rate equation to represent the electrochemical reaction at the reaction channel and an analogue of the solution of the diffusion equation. The experimental data were well reproduced by the propagation model. The electronic conductivity is concluded to be an origin to generate the inhomogeneous progress of the electrode reaction in the LIB cathode sheet.

Acknowledgement

A part of this work was supported by JSPS KAKENHI Grant Number JP15K17924. The development of the VDXAFS instrument was supported by the RISING project of New Energy and Industrial Technology Development Organization (NEDO). The VDXAFS measurements were performed under the approval of Photon Factory Program Advisory Committee (Proposal No. 2014G542).

References

[1] H. H. Chang, C. C. Chang, H. C. Wu, M. H. Yang, H. S. Sheu, and N. L. Wu, *Electrochem. Commun.*, **10**, 335 (2008).

[2] A. Deb, U. Bergmann, S. P. Cramer, and E. J. Cairns, *Electrochim. Acta*, **50**, 5200 (2005).

[3] C. Delmas, M. Maccario, L. Croguennec, F. L. Cras, and F. Weill, *Nat. Mater.*, **7**, 665 (2008).

[4] Y. Orikasa, T. Maeda, Y. Koyama, H. Murayama, K. Fukuda, H. Tanida, H. Arai, E. Matsubara, Y. Uchimoto, and Z. Ogumi, *J. Am. Chem. Soc.*, **135**, 5497 (2013).

[5] J. B. Leriche, S. Hamelet, J. Shu, M. Morcrette, C. Masquelier, G. Ouvrard, M. Zerrouki,

P. Soudan, S. Belin, E. Elkaïm, and F. Baudelet, *J. Electrochem. Soc.*, **157**, A606 (2010).
[6] S. Tobishima and J. Yamaki, *J. Power Sources*, **81**, 882 (1999).
[7] M. Katayama, K. Sumiwaka, K. Hayashi, K. Ozutsumi, T. Ohta, and Y. Inada, *J. Synchrotron Rad.*, **19**, 717 (2012).
[8] M. Katayama, K. Sumiwaka, R. Miyahara, H. Yamashige, H. Arai, Y. Uchimoto, T. Ohta, Y. Inada, and Z. Ogumi, *J. Power Sources*, **269**, 994 (2014).
[9] G. Ouvrard, M. Zerrouki, P. Soudan, B. Lestriez, C. Masquelier, M. Morcrette, S. Hamelet, S. Belin, A. M. Flank, and F. Baudelet, *J. Power Sources*, **229**, 16 (2013).
[10] J. Nanda, J. Remillard, A. O'Neill, D. Bernardi, T. Ro, K. E. Nietering, J. Y. Go, and T. J. Miller, *Adv. Funct. Mater.*, **21**, 3282 (2011).
[11] M. Katayama, R. Miyahara, T. Watanabe, H. Yamagishi, S. Yamashita, T. Kizaki, Y. Sugawara, and Y. Inada, *J. Synchrotron Rad.*, **22**, 1227 (2015).